

Yeast screens show aromatic residues at the end of the sixth helix anchor transient receptor potential channel gate

Xinliang Zhou*, Zhenwei Su*, Andriy Anishkin†, W. John Haynes*, Eric M. Friske*, Stephen H. Loukin*, Ching Kung**§, and Yoshiro Saimi**§

*Laboratory of Molecular Biology and †Department of Genetics, University of Wisconsin, Madison, WI 53706; and ‡Department of Biology, University of Maryland, College Park, MD 20742

Edited by David Julius, University of California, San Francisco, CA, and approved August 9, 2007 (received for review May 1, 2007)

Transient receptor potential (TRP) channels are first elements in sensing chemicals, heat, and force and are widespread among protists and fungi as well as animals. Despite their importance, the arrangement and roles of the amino acids that constitute the TRP channel gate are unknown. The yeast TRPY1 is activated *in vivo* by osmotically induced vacuolar membrane deformation and by cytoplasmic Ca^{2+} . After a random mutagenesis, we isolated TRPY1 mutants that responded more strongly to mild osmotic upshocks. One such gain-of-function mutant has a Y458H substitution at the C terminus of the predicted sixth transmembrane helix. Direct patch-clamp examination of vacuolar membranes showed that Y458H channels were already active with little stimulus and showed marked flickers between the open and intraburst closed states. They remained responsive to membrane stretch force and to Ca^{2+} , indicating primary defects in the gate region but not in the sensing of gating principles. None of the other 18 amino acid replacements engineered here showed normal channel kinetics except the two aromatic substitutions, Y458F and Y458W. The Y458 of TRPY1 has its aromatic counterpart in mammalian TRPM. Furthermore, conserved aromatics one α -helical turn downstream from this point are also found in animal TRPC, TRPN, TRPP, and TRPML, suggesting that gate anchoring with aromatics may be common among many TRP channels. The possible roles of aromatics at the end of the sixth transmembrane helix are discussed.

aromatic residue anchoring | gating machinery | mechanosensitivity | yeast calcium signal | vacuolar membrane

The transient receptor potential (TRP) superfamily encompasses a diverse group of nonspecific cation channels, each responding to multiple stimuli (1). Sequence similarity among all members of the TRP superfamily is limited to only the fifth transmembrane helix (TM5) through the sixth transmembrane helix (TM6). Comparisons therein show that animal TRP subtypes are no more related to each other than they are to fungal or protist TRP subtypes. TRPY1, the sole TRP homolog in the budding yeast *Saccharomyces cerevisiae*, forms a stretch-activated cation channel of 320-pS conductance that is located in the vacuolar membrane (2–4). Osmotic upshocks activate TRPY1 to release Ca^{2+} to the cytoplasm (4). The released Ca^{2+} further activates TRPY1 in a Ca^{2+} -induced Ca^{2+} release (CICR) feedback (2) and can be monitored by the luminescence of transgenic aequorin as a phenotype (4), which is valuable in mutant screening. Furthermore, the TRP channels on the yeast vacuole can be directly examined *in situ* under a patch clamp (2, 3, 5). In contrast, animal TRP channels in complex organs and tissues are often difficult to access. Patch-clamp examinations of animal TRP channels, when possible, are carried out heterologously, except for TRPC1 (6). To complement this effort, using animal models, we combined molecular genetics and patch-clamp electrophysiology to analyze the structure–function relationship of yeast TRP channels.

Results

Mutant Screening Based on an Osmotically Induced Ca^{2+} Signal. We randomly mutagenized the entire ORF of TRPY1 and screened $\approx 4,000$ yeast lines for mutants showing an unusually strong Ca^{2+} luminescence [gain-of-function (GOF)] phenotype. Such mutants were further examined under patch clamp because their higher sensitivity to the test osmotic shock makes them candidates for harboring constitutively active channels (Fig. 1*a*). Our first harvest yielded 10 GOF mutations distributed one each in the predicted N-terminal cytoplasmic domain (I195T), TM1 (F247L), TM3 (S297W), TM5 (F380L), and the P-loop (G402S); two in TM6 (Y442C and Y458H); and three in the C-terminal cytoplasmic domain. Of the last three, two are at the same residue near TM6 (Y473H and Y473C) and one is further out (E501K). Thus, there is a preponderance of mutations affecting aromatic residues among the ten GOF mutations and possibly a concentration of mutations at or near the cytoplasmic end of TM6. We sequenced randomly picked clones from the mutagenized but unselected population to see whether mutations at or near TM6 originated from a mutagenesis bias or from selection; 22 mutations found among unselected clones were distributed throughout the gene, showing no mutational hot spots and no preponderance of aromatic mutations. Preliminary patch-clamp examinations showed that all 10 mutations affected channel kinetics and open probability differently. The mutant with the Y458H substitution at the cytoplasmic end of TM6 (Fig. 1*b*) has the most severe electrophysiological phenotype and is the subject of this work. Gauging by the Ca^{2+} luminescence, the Y458H cells clearly responded more strongly than the wild type to a large range of upshocks (Fig. 1*c* and *d*).

Single-Channel Electrophysiological Analyses of the Y458H TRPY1.

Under patch clamp, the unitary conductance measured in symmetric 180 KCl was 322 ± 11 pS for the wild type and 310 ± 9 pS for the Y458H (mean \pm SD, $n = 3$). Based on reversal potentials, the permeability ratios of mono- and divalent cations were as follows for both channels: $P_{\text{K}^+}/P_{\text{Na}^+}/P_{\text{Mg}^{2+}}/P_{\text{Ca}^{2+}} = 1:1:0.41:0.33$. These ratios indicate that the lining of the ion pathway, including the filter, was intact. Averaged channel

Author contributions: X.Z. and Z.S. contributed equally to this work; C.K. and Y.S. designed research; X.Z., Z.S., A.A., W.J.H., E.M.F., and S.H.L. performed research; and C.K. and Y.S. wrote the paper.

The authors declare no conflict of interest.

This article is a PNAS Direct Submission.

Abbreviations: TRP, transient receptor potential; TM n , n th transmembrane helix; GOF, gain-of-function; P_o , open probability.

§To whom correspondence should be addressed at: Laboratory of Molecular Biology, University of Wisconsin, 1525 Linen Drive, Madison, WI 53706. E-mail: ckung@wisc.edu or ysaimi@wisc.edu.

This article contains supporting information online at www.pnas.org/cgi/content/full/0704039104/DC1.

© 2007 by The National Academy of Sciences of the USA

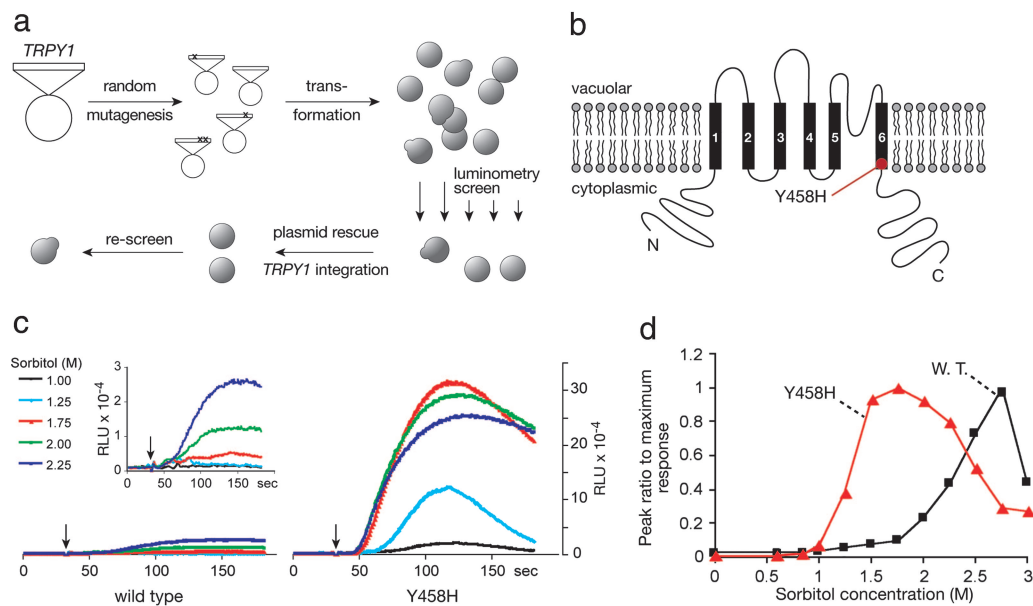


Fig. 1. Isolation and the *in vivo* phenotype of a TRPY1 GOF mutant. (a) Procedure for mutant screening. (b) Locations of the severe GOF mutation mapped onto the predicted membrane topology of a TRPY1 subunit. (c) Responses of populations of live yeast cells to the addition (at second 30, arrows) of sorbitol at different concentrations as monitored through the luminescence, in relative luminescence units (RLU) per second, of transgenic aequorin. The responses of Y458H (Right) were much stronger than those of the wild type (Left), which was also evident after a $\times 10$ magnification (Inset). (d) Peak responses to different sorbitol concentrations relative to the highest peak observed. The leftward shift indicates that Y458H is hypersensitive. These results were typical of three full test sets.

density in whole vacuole or in excised patches also appeared to be unaltered. However, the mutant displayed prominent defects in gating kinetics ($n > 30$ preparations). At 10^{-5} M Ca^{2+} , the unitary conductances of a wild-type whole-vacuole ensemble were clearly resolved (Fig. 2a Left), whereas the Y458H ensemble current rapidly flickered from the all-open level, giving a noisy impression (Fig. 2a Center). Such “noise” can nonetheless be shown to comprise unitary activities after thinning the ranks in the ensemble by lowering the $[\text{Ca}^{2+}]$ (Fig. 2a Right). The pronounced kinetic difference is better resolved with excised patches, cytoplasmic side out, each containing a single unit. The open probability (P_o) of the mutant was much higher than that of the wild type at the same $[\text{Ca}^{2+}]$. Without added pressure, the wild-type channels were active only at or above 10^{-6} M Ca^{2+} (Fig. 2b Left), whereas the mutant channel was active even at 10^{-7} M Ca^{2+} (Fig. 2b Right). At 10^{-6} M Ca^{2+} , the wild-type P_o was only ≈ 0.03 , whereas that of the mutant was ≈ 0.5 . The increased P_o , together with the kinetic changes (see below), indicate that Y458H destabilizes the closed state. At a P_o of ≈ 0.4 (at 5×10^{-6} M Ca^{2+}), most (62%) of the openings of the wild-type channel were longer than 10 msec ($\tau \approx 70$ msec, $n = 3$, Fig. 2c Upper Left). For the Y458H channel at a comparable P_o of ≈ 0.4 (at 5×10^{-7} M Ca^{2+}), the openings were frequently interrupted. Most (95%) of the openings were shorter than 10 msec, and even the long openings were shortened ($\tau \approx 8$ msec, Fig. 2c Lower Left). Approximately half (54%) of the closures of the wild-type TRPY1 were long ($\tau \approx 153$ msec, $n = 3$, Fig. 2c Upper Right). Like the open time, the closed time distribution of Y458H also showed a prominent left shift (Fig. 2c Right). Although longer interburst closures could still be discerned ($\tau \approx 55$ msec, $n = 3$), they accounted for $< 5\%$ of the events (Fig. 2c Lower Right). Pressure pulses activated the wild-type channels in excised patches with the cytoplasmic side out (7) (Fig. 2d Upper, at 10^{-6} M Ca^{2+}). At $[\text{Ca}^{2+}]$ commonly used for testing, P_o values of Y458H were already very high even without pressure (Fig. 2b). At 10^{-7} M Ca^{2+} , the Y458H channels showed clear responses to pressure applied through the pipette (Fig. 2d). However, seals and patches responded erratically to pressure at this low $[\text{Ca}^{2+}]$,

making quantification unreliable. Therefore, we cannot conclude whether the mutation affects the channel’s response to unit force change. However, the large response to osmotic upshock *in vivo* is best explained by the observed large increase in P_o under any conditions tested (see Discussion). In short, the key effect of the Y458H mutation is in destabilizing the gate to raise the P_o in general, giving the appearance of the channel’s being more sensitive to the gating stimuli (cytoplasmic Ca^{2+} and stretch force).

Only Aromatic Amino Acids at Position 458 Maintain Gate Stability.

Because of our findings with Y458H, we engineered all 18 other substitutions at Y458 to examine the chemical basis of gate destabilization. Several substitutions (Y458D, Y458E, Y458K, Y458R, and Y458T) rendered patches silent or nearly so, presumably reflecting severe channel malfunctions. Other substitutions (Y458A, Y458C, Y458G, Y458I, Y458L, Y458M, Y458N, Y458Q, Y458S, Y458P, and Y458V) gave channels with clear kinetic abnormalities indicative of closed- and open-state alterations to different degrees ($n = 3$ –5 each; see the bottom five traces in Fig. 3). Only the two aromatic substitutions Y458F and Y458W retained the wild-type-like kinetics (Fig. 3, top two traces).

Similar Aromatics in Animal TRP Channels. We note that Y458 has its aromatic counterparts in fungal homologs and in mammalian TRPMs. Aromatics are also found downstream from this point, spaced by three residues, in many but not all of vertebrate TRP channels (Fig. 4). Residues with such a spacing in an α -helix have the same aspect, likely facing the same environment.

Discussion

There is surprisingly little concrete knowledge on the gates of TRP channels, given their importance and the current interest in them. Because the predicted membrane topology of TRP subunits is similar to that of *Shaker*-type K^+ channels, structural similarity is assumed, even though sequence similarity is limited between TRP and *Shaker* channels. Our main finding is that the

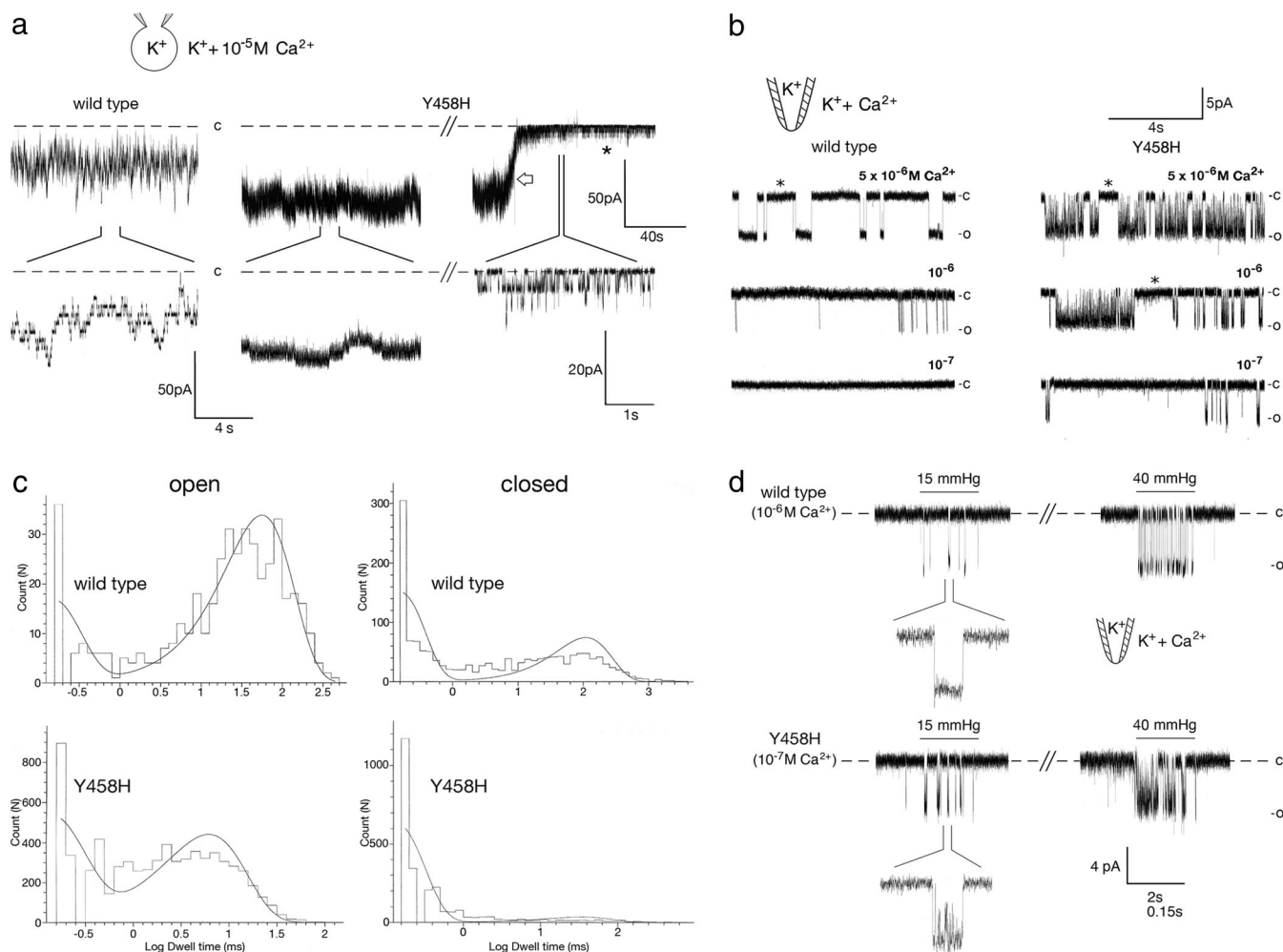


Fig. 2. Kinetics of wild-type and Y458H TRPY1. All currents presented flow into the cytoplasm and are shown downward from the closed level indicated by "c." (a) Ensemble currents from whole vacuoles bathed in 10^{-5} M Ca^{2+} . Unlike the wild-type current (Left), the Y458H channels (Right) have high P_o , and the ensemble current flickers near the all-open level (Center). The discrete unitary nature of the mutant current (Right, indicated by an asterisk) is best seen after the units in the same ensemble were reduced by lowering the $[\text{Ca}^{2+}]$ by perfusion (indicated by an arrow). (b) Behavior of single units each in excised patches with the cytoplasmic side out. The mutation does not alter the unitary conductance. c, Closed; o, open level. The flickering behavior of the mutant channel is evident when compared with the wild type at any $[\text{Ca}^{2+}]$. The P_o of the mutant channel is higher at all but the saturating $[\text{Ca}^{2+}]$. Interburst closures (indicated by asterisks) remain observable in the mutant. (c) Dwell-time distributions each with a two-exponential fit ($n = 3$). The open times of the wild type at 5×10^{-6} M Ca^{2+} (Upper Left) show a prominent dwell time, $\tau = 70.0 \pm 11.2$ ms, accounting for 62% of the opening events. For Y458H at 5×10^{-7} M Ca^{2+} (Lower Left), a similar 61% of the openings are shortened to $\tau = 8.2 \pm 2.3$ msec. For the wild type at 5×10^{-6} M Ca^{2+} (Upper Right), 54% of the closures are of the long form with a dwell time of $\tau = 153 \pm 37$ msec. Long (interburst) closures, although shortened to $\tau = 55 \pm 19$ msec, are discernable in Y458H, but account for only 5% of the events. (Lower Right) 95% of the closures are shorter than 10 msec. (d) Mechanosensitivity of the wild-type and Y458H channels. Applied positive pressure pulses to the excised patches activate both channels. The stretch-activated Y458H channel retains its characteristic flickers as shown time-expanded in lower traces. Note that the bath $[\text{Ca}^{2+}]$ was adjusted to ease comparison.

aromaticity of a residue at the cytoplasmic end of TM6 is crucial in maintaining normal gating kinetics of TRPY1. The finding suggests that this aromatic residue is in a special stereochemical environment and may be near the gate proper, which is likely the result of the convergence of the cytoplasmic end of TM6, much like that of *Shaker*. A computational model, based on limited homology to known K^+ channel structures, can be found in the supporting information (SI) Fig. 5 and SI Methods.

Mutations that increase channel P_o are rare but have been recovered in yeast screens of a native (8) and a foreign (9, 10) K^+ channel. Disease or experimental point mutations reported to date all cause reduction or loss of TRP channel activities, including the dominant polycystic kidney disease (PKD) alleles (11) and a dominant-negative construct of TrpV1 (12). The Y458H GOF mutation is also a rare find even in our experiment. Here, each of TRPY1's 685 residues has a chance of being

mutated to other varieties. Among the 10 GOF mutants selected from 4,000 lines and biophysically examined to date, Y458H is the one showing the most severe gate destabilization. Y458H mutant cells clearly respond more strongly to milder osmotic upshocks (Fig. 1 c and d). *A priori*, this apparent increase in sensitivity to upshock *in vivo* may reflect the mutant channel's stronger tendency to open under all conditions or its being more sensitive to unit change in membrane tension, or both. We found the P_o of the mutant to be egregiously large in most circumstances (Fig. 2). This phenotype and the patch instability under pressure at low $[\text{Ca}^{2+}]$ confound a direct comparison of how the Y458H channels respond to unit force. Although we cannot be certain that this is the only reason, the simplest interpretation is that the GOF phenotype *in vivo* results from the large increase in P_o under any conditions because of the defect in its gate. One may wonder why the ground level of Ca^{2+} luminescence before

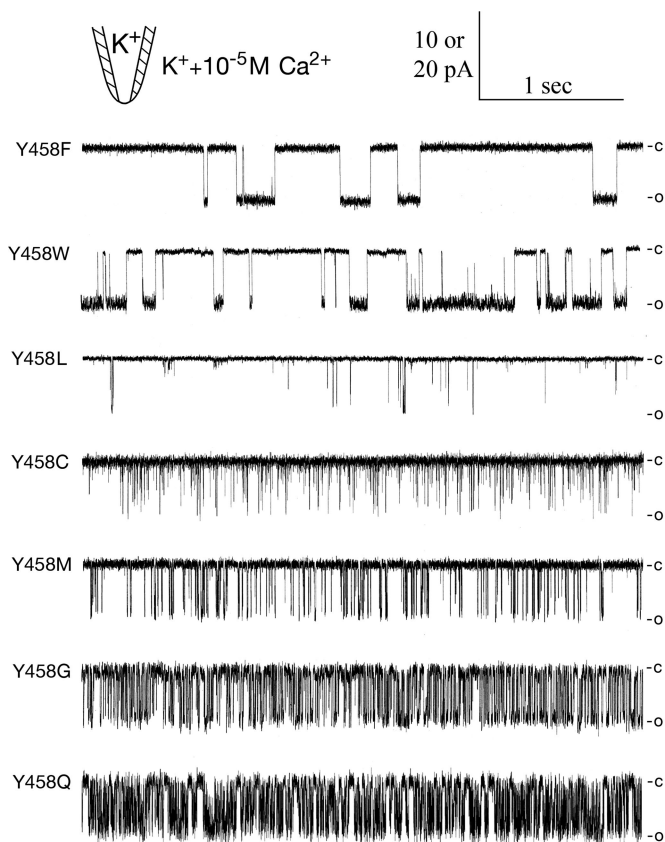


Fig. 3. Activities of TRPY1 channels with various substitutions at residue 458. Records from excised patches bathed in 10^{-5} M Ca^{2+} , each apparently with a single unitary conductance, are presented to ease direct comparison. Among all substitutions, only Y458F and Y458W (top two traces) show single-channel kinetics that resemble the wild type. $P_o = 0.5 \pm 0.2$, 0.1 ± 0.1 , and 0.6 ± 0.2 ; $\tau_{\text{open}} = 81 \pm 13$, 128 ± 17 , and 61 ± 14 msec, for the wild type Y458, and mutant Y458F and Y458W, respectively; mean \pm SD ($n = 3$ each). Aberrant gatings are evident in other substitutions. Shown are Y458L, Y458C, Y458M, Y458G, and Y458Q (bottom five traces). $P_o < 0.1$ for Y458L and Y458C, $P_o = 0.1$ for Y458M, $P_o = 0.3$ for Y458G, and $P_o = 0.6$ for Y458Q; $\tau_{\text{open}} < 1.5$ msec for Y458L, Y458C, Y458M, and Y458Q; $\tau_{\text{open}} = 3 \pm 0.9$ msec for Y458G ($n = 3$ each). Recording was performed at -30 mV, except in the case of Y458L, which was performed at -60 mV. Calibration was 1 sec and 10 pA (20 pA for Y458L). See Fig. 2 for comparison with the wild type and Y458H.

the osmotic upshock indicated by aequorin is not higher in the mutant (Fig. 1c). There may be inhibitory mechanisms that eventually shut off Y458H channels *in vivo* by using chemistry or in long durations not tested in our patch-clamp examinations. Even if the mutant channel leaks Ca^{2+} at all times, it may not necessarily affect the level of cytosolic $[\text{Ca}^{2+}]$. Ca^{2+} homeostasis in the cytoplasm is complex and involves reuptake components and release components in mutual feedback control. The reuptake activities of the Ca^{2+} pump (Pmr1p) and the $\text{Ca}^{2+}/\text{H}^+$ exchanger (Vcx1p) are known to increase when cytosolic $[\text{Ca}^{2+}]$ is high to prevent Ca^{2+} toxicity. Their activities could mask the leak from the Y458H TRPY1 channel, if there was one.

The fact that only the aromatic residues (tyrosine, phenylalanine, and tryptophan) of the 20 variations at position 458 maintain the gate's stability is not likely a coincidence. This aromaticity requirement indicates that position 458 at the cytoplasmic end of TM6 must be in a special stereochemical environment to stabilize the open and/or closed states. Aromatic interactions among protein domains define structures, such as the cuff surrounding the K^+ filter in *kcsA* (13). Three belts of interacting aromatics can be recognized in KirBac1.1 (14).

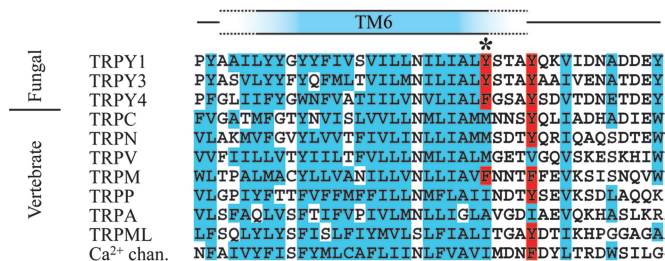


Fig. 4. An alignment of the predicted TM6 and its proximal C-terminal extension. A ClustalW alignment (Gonnet 250 matrix) was produced by using the ClustalX (version 1.81) Windows interface (21). Aromatic and conserved hydrophobic residues are shaded blue. The asterisk marks the position of Y458 in TRPY1. Aromatic residues frequently occur one α -helical turn downstream from this point in both fungal and vertebrate channels (shaded red). TRPY3 was from *Candida albicans* (infectious yeast); TRPY4 was from *Cryptococcus neoformans* (agent of cryptococcosis); TRPN (NOMPC-2) was from *Danio rerio* (zebra fish); TRPC5-1, TRPM1-1, TRPV4-1, TRPA1, TRPP (PKD2), TRPML-1 and the end of the fourth repeat of L-type Ca channel were all from human.

Aromatic amino acids are also known to interact with lipids and prefer to locate the lipid-water interface (15, 16). In model peptides, they resist being displaced from that interface (17). In a simulation, aromatics of KirBac1.1 align more sharply at the interface after opening (14), suggesting their roles in stabilizing the open form and in preventing dwells in intermediate forms during conformational changes. Here, the consequence of losing such aromatic anchors is vividly displayed as an *in vivo* phenotype (Fig. 1) and as single-channel activities (Figs. 2 and 3). As shown in Fig. 4, TRPY1's Y458 has its direct aromatic counterpart in TRPM. Furthermore, immediately downstream in the α -helix is another aromatic residue that is common to most members of the TRP superfamily. It would be interesting to test whether Y462 and Y473 of TRPY1, as well as their counterparts in animal TRP channels, also serve as gate anchors.

Materials and Methods

Mutagenesis and Luminometric Phenotyping. Mutant selection proceeded in two steps: First, TRPY1-bearing plasmids were mutagenized and *trpy1* Δ transformants were subjected to the initial rounds of selection. Subsequently, the insert from each of the selected plasmids was excised, subcloned, and eventually inserted into the yeast chromosome by gene replacement for the final round of selection and characterization. This two-step procedure is necessary because the spheroplasts for patch clamping need to be prepared in a nonselective medium in which the *trpy1*-bearing plasmid may be evicted. At the same time, gene replacement cannot be carried out *en masse* before selection, in numbers suitable for nondirected mutageneses.

Originally derived from HA-tagged TRPY1 (18) in p416GALL (American Type Culture Collection, Manassas, VA), the plasmid TRPY1-HA, which contains a weakened *GAL1* inducible promoter and a *URA* marker between the ORF and the 3' UTR of TRPY1, was mutagenized by passing through mutator XL1-Red Cells (Invitrogen, Carlsbad, CA). Pots of independently mutagenized plasmids were transformed into Stanford deletion strain BY4742 ($\Delta trpy1$) with pEVP11/AEQ plasmid bearing the *apoeaquorin* gene (19). Transformants were selected on complete minimum dropout (CMD)-u-1 plates (minimum dextrose medium with uracil and leucine dropout) (20). Colonies were picked and cultured in forty 96-well microplates with liquid CMD-u-1 medium. After a few days of growth, frozen stocks were made. Culture from each well ($5 \mu\text{l}$) was transferred into $45 \mu\text{l}$ of DCGR (DCGR was the same as CMD-u-1 except ammonium chloride was substituted for sulfate and galactose and raffinose were substituted for glucose) with 0.5 or $1 \mu\text{M}$ of coelenterazine in fresh microplates and cultured

overnight. For luminescence measurement, the microplate was read by using a Mithras LB940 microplate reader (Berthold Technologies, Bad Wilbad, Germany). Five seconds into the reading, 50 μ l of hypertonic solution (1.5 M sorbitol in DCGR) was added, and luminescence was measured continually for another 35 sec. Putative mutants with stronger responses were rescreened following the same procedure with a Berthold LB9507 luminometer. The plasmids of those passing the rescreen were retrieved, sequenced, restricted, and inserted into a plasmid for gene replacement containing the *TRPY1* 5' and 3' UTRs and the *URA3* marker. This fragment (5' UTR/*TRPY1* ORF/*URA3*/3' UTR), released after digestion with *EagI* and *HpaI*, was used to transform BY4742 (Δ *trpy1*) yeast, and the integrants, selected through *URA*⁺, were sequenced and confirmed to contain the original mutations. Each integrant was then screened by luminometry again for the effect of the mutation. The final luminometric assay was similar to those of Denis and Cyert (4), except that cells were cultured without agitating the vessels. Twenty microliters of culture in CMD-u-1 with ammonium chloride at OD₆₀₀ of 4.2 was shocked with 200 μ l of various concentrations of 0–3 M sorbitol in the same medium. The mutagenic rate was assessed in MH1066 bacteria, as previously

described (8). The loss of prototrophy was 2–3% in the present work. No mutational hot spots were observed at the nucleotide level. As described in *Results*, 10 selected strong GOF mutations showed no protein-domain preference. Seven mutations with weak phenotypes also showed no domain preference.

Patch Clamp. Preparations of spheroplasts and vacuoles as well as patch-clamp procedures were as previously described (2). Data acquisition, analysis, and fitting to exponential probability density functions were performed by using Axon Instruments (Union City, CA) pCLAMP 9 system. Symmetric solutions contained 150 mM KCl and various [Ca²⁺] buffered with 1 mM 1,2-bis(2-aminophenoxy)ethane-*N,N,N',N'*-tetraacetate (BAPTA) as well as 5 mM Hepes at pH 7.2. Recording was performed at –30 mV (cytoplasmic side negative) unless specified. Pressures were applied through a syringe and gauged with a manometer. The electrode pipette had a bore size of \approx 1 μ m in diameter. Data were acquired at 10 kHz and filtered at 2 kHz.

This work was supported by National Institutes of Health Grants GM054867 (to Y.S.) and GM047856 (to C.K.) and by the Vilas Trust of the University of Wisconsin, Madison.

1. Clapham DE (2003) *Nature* 426:517–524.
2. Zhou XL, Batiza AF, Loukin SH, Palmer CP, Kung C, Saimi Y (2003) *Proc Natl Acad Sci USA* 100:7105–7110.
3. Palmer CP, Zhou XL, Lin J, Loukin SH, Kung C, Saimi Y (2001) *Proc Natl Acad Sci USA* 98:7801–7815.
4. Denis V, Cyert MS (2002) *J Cell Biol* 156:29–34.
5. Saimi Y, Martinac B, Delcour AH, Minorsky PV, Gustin MC, Culbertson MR, Adler J, Kung C (1992) *Methods Enzymol* 207:681–691.
6. Maroto R, Raso A, Wood TG, Kurosky A, Martinac B, Hamill OP (2005) *Nat Cell Biol* 7:179–185.
7. Zhou XL, Loukin SH, Coria R, Kung C, Saimi Y (2005) *Eur Biophys J* 34:413–422.
8. Loukin SH, Vaillant B, Zhou XL, Spalding EP, Kung C, Saimi Y (1997) *EMBO J* 16:4817–4825.
9. Yi BA, Lin YF, Jan YN, Jan LY (2001) *Neuron* 29:657–667.
10. Sadja R, Smadja K, Alagem N, Reuveny E (2001) *Neuron* 29:669–680.
11. Nauli SM, Zhou J (2004) *Bioessays* 26:844–856.
12. Kuzhikandathil EV, Wang H, Szabo T, Morozova N, Blumberg PM, Oxford GS (2001) *J Neurosci* 21:8697–8706.
13. Doyle DA, Morais Cabral J, Pfuetzner RA, Kuo A, Gulbis JM, Cohen SL, Chait BT, MacKinnon R (1998) *Science* 3:69–77.
14. Domene C, Vemparala S, Klein ML, Venien-Bryan C, Doyle DA (2006) *Biophys J* 90:L01–3.
15. Braun P, von Heijne G (1999) *Biochemistry* 38:9778–9782.
16. Gaede HC, Yau WM, Gawrisch K (2005) *J Phys Chem B* 109:13014–13023.
17. Demmers JA, van Duijn E, Haverkamp J, Greathouse DV, Koeppe RE, II, Heck AJ, Killian JA (2001) *J Biol Chem* 276:34501–34508.
18. Lin J (2002) PhD dissertation (University of Wisconsin, Madison).
19. Batiza AF, Schulz T, Masson PH (1996) *J Biol Chem* 271:23357–23362.
20. Ausubel FM, Brent R, Kingston RE, Moore DD, Seidman JG, Smith JA, Struhl K (1995) *Current Protocols in Molecular Biology* (Wiley & Sons, New York).
21. Thompson JD, Gibson TJ, Plewniak F, Jeanmougin F, Higgins DG (1997) *Nucleic Acids Res* 25:4876–4882.